Synthesis and Characterization of Photoconducting Polyaniline–TiO_2 Nanocomposite

Wei Feng,# Enhai Sun,†† Akihiko Fujii, Hongcai Wu,† Koichi Niihara,†† and Katsumi Yoshino*

Department of Electronic Engineering, Graduate School of Engineering, Osaka University, 2-1 Yamada-Oka, Suita, Osaka 565-0871

†School of Electronic and Information Engineering, Xi'an Jiaotong University, Xi'an, 710049, P.R.China

††Institute of Scientifical and Industrial Research, Osaka University, 2-9 Mihokaoka, Ibaraki, Osaka 567-0047

(Received June 21, 2000)

A composite of polyaniline (PANI) encapsulating titanium oxide (TiO_2) with nanometer size has been synthesized by in-situ emulsion polymerization. Particle dimensions have been measured and the nature of the association between the components have been observed using SEM and TEM techniques. The interaction between PANI and TiO_2 and the nature of chain growth have been investigated and explained according to the results of FTIR. The improvement of thermal stability and crystallinity of nanocomposites have been evaluated by using TGA and XRD. The mechanism of charge transport in these composites has also been studied by measuring the DC conductivity of all samples and the temperature-conductivity relation. The photoconductivity of PANI–TiO_2 composite has been enhanced markedly. This effect is discussed by taking the photoinduced charge transfer between PANI and TiO_2 into consideration.

Conducting polymer composites (CPC) are, in fact, some suitable composition of a conducting polymer with one or more insulating materials so that their desirable properties are combined successfully. Interest in the development of new inorganic-polymer composite materials of the nanometer scale has grown in recent years due to a wide range of potential uses of the composite in microelectronics, display technologies, and catalysis and sensor.[1—3] These materials are especially important owing to their bridging role between the world of conducting polymers and that of nanoparticles. Some novel properties such as photosensitivity[4] and positive temperature coefficient (PTC) of resistance[5] have been found in these nanocomposites. Among various conducting polymers, polyaniline (PANI) has been of particular interest because of its diverse structures, special doping mechanism, excellent environmental stability, good solution processability and wide applications as electronic materials.[6] PANI has been successfully utilized in preparations of different nanocomposites with different purpose such as PANI–TiO_2,[5] PANI–MoO_3,[7] PANI–HUO_2PO_4,[8] PANI–V_2O_5,[9] PANI–Fe_2O_3,[10] PANI–SiO_2,[11] PANI–SnO_2[12] and PANI–$BaSO_4$.[13] Most of the studies so far published deal with the conductivity of such nanocomposites. The morphology of PANI–TiO_2 nanocomposites as well as the nature of association between the components, however, has been studied only to a limited extent.[5] Somani et al. reported about the morphological characteristics of PANI-TiO_2 nanocomposite, but detailed studies and the photovoltaic characteristic determinations have not been carried out yet.

In this study, we report the in-situ emulsion polymerization of a TiO_2 encapsulated PANI nanocomposite, utilizing the functionalized protonic acid, dodecylbenzene sulfonic acid (DBSA), as both a dopant and a surfactant, to form the aqueous emulsion system. TiO_2 particles act as the reaction core and polyaniline is formed preferentially on the surface of TiO_2 particles. TiO_2, rather than being simply blended or mixed up, are encapsulated or entrapped into the conducting polymer core, resulting in some significant improvement in different physical properties of the conducting polymers. The composite size can be controlled by means of TiO_2 content added in the reaction system. The SEM and TEM studies are undertaken to determine the particle size as well as the nature of association between the two components. Thermal stability, crystallinity, electrical conductivity, temperature-conductivity relation and photoconductivity of the samples are studied in the course of the work.

Experiments

Materials: TiO_2 powder (P25) was donated by Degussa AG, Frankfurt, in the form of 30% rutile and 70% anatase, with an average particle size of approximately 21 nm. Aniline was vacuum-distilled and kept in the dark prior to use. All other solvents and chemicals were analyzing reagent grade and were obtained from Nacalai tesque, Japan.

Preparation of the Nanocomposites: Aniline-DBSA complex was prepared by mixing aniline (0.4 g) and DBSA (1.44 g), of stoichiometric ratio, in water (30 g) for 30 min, till a white emulsion of An-DBSA was obtained. The solution was precooled at 0 °C and the desired quantity of TiO_2 was added to the reaction system; this mixture was stirred

Xi'an Jiaotong University

throughly for 2 h. A solution of ammonium peroxydisulfate (APS) (0.98 g dissolved in 5 g water) was added dropwise. The polymerization process was carried out at 0 °C for 5 h. A color change from white through pale green (after an induction period of 120 min) to deep green was observed. At the end of polymerization, a green and very stable aniline-DBSA-TiO_2 dispersion was obtained. Methanol was added to the above aqueous dispersion to precipitate the composite powder. The precipitate was filtered and washed with methanol and dried in a vacuum oven (40 °C, 4 h). The color of the powder and the size of the particle obtained vary depending on the TiO_2 content. The PANI–TiO_2 composites with 0%, 11%, 33%, 47% and 61% TiO_2 weight content were marked by S_0, S_1, S_2, S_3 and S_4, respectively. The physical properties of composites are shown in Table 1.

Preparation of Undoped PANI–TiO_2 Composite Film: Undoped PANI-TiO_2 composite was prepared by mixing S_2 powder and a 1.0 M NH_3 aqueous solution at room temperature for 2 h (M = mol dm^{-3}). The resultant undoped nanocomposite was filtered, washed throughly and vacuum dried at 40 °C for 2 h.

1 g undoped S_2 powder was dissolved in 70 ml *N*-methyl-2-pyrrolidone (NMP) solvent and the resultant solution was spin-coated on transparent conducting ITO-coated glass substrates with aluminum (Al) contacts evaporated on the top, with a portion of the ITO removed for making electrical contact to the Al.

Characterization: Measurements of particle sizes of PANI–TiO_2 composites and observations of the nature of association between the TiO_2 and PANI were performed using a Hitachi 8000 transmission electron microscope and a Hitachi S-2100A scanning electron microscope. Fourier Transform Infrared Spectroscopy (FTIR measurement) of the composite was carried out on a JASCO corporation FT/IR-300E. Thermal gravimetric analysis (TGA) was carried out on a SEIKO I & E SSC/570 Thermal controller and a TG/DTA 30 at a heating rate of 10 °C min^{-1} in air. X-ray diffraction measurements using Cu $K\alpha$ radiation were performed with a powder X-ray diffractometer (RINT 1100, Rigaku). A small quantity (40 mg) of the powder was compacted at 29.4 MPa pressure in order to make thin disc pellets for electrical and density measurements. The conductivity of the pellet was measured by four probe method over a temperature range from −70 °C to 27 °C using a programmable DC voltage/current generator (Keithley 617). Gold and aluminum electrodes were used for contacts which were coupled to the digital electrometer. Absorption was measured using a Hitachi 330 UV-vis spectrophotometer. Photoelectrical measurements were carried out in a vacuum optical cryostat in a vacuum of about 10^{-5} Torr (1 Torr ≈ 133.322 Pa). Current-voltage characteristics were measured using a Keithley 617 picoammeter. A high-intensity Xenon lamp (500 W) was used as an UV-vis light source. The spectral response of the device was corrected for the response of the lamp-monochromator system by measuring the calibration spectrum with an UV-enhanced Si photodiode placed in the sample position.

Results and Discussion

In order to determine the particle sizes of PANI–TiO_2 composites and to observe the nature of association between the PANI and TiO_2, samples were studied by SEM and TEM, respectively. For comparative study, the electron beam parameters were kept constant while analyzing all samples. Figures 1a and 1b are the typical SEM images of S_1 and S_3, respectively. The SEM images show clearly that the dimension of PANI–TiO_2 composite is in the range of 40—60 nm in diameter, centered at 50 nm. It is also clear in this figure that in the PANI–TiO_2 composite a great number of globules of 40—60 nm in diameter are heaped together. It has been reported that the morphology of the composites does not differ much from that of pure PANI,[14] however, as the TiO_2 content increases, the particle size becomes smaller and smaller, which leads to the changes of the surface morphological structure of heaped composites from loose cotton to firm gravel in appearance. Figures 1c and 1d are the TEM images of S_2, S_3 and Figs. 1e, 1f, and 1g are the diffraction patterns of S_2 in different sites of some composite particles. The apparent physical nature of PANI changes remarkably after composite formation: the initial fibre-like texture[15] changes to a distinctly shaped granular form. Concerning TiO_2 particles, there are polydisperse spheres lying in the size range of 20 nm. After composite formation, these particles are found to be entrapped in PANI chain leading to the increase of the particle size. Therefore, the TiO_2 particles are not simply mixed up or blended with the PANI, but they are rather glued or bound by the PANI chains. The diffraction pattern Fig. 1e, which diffracted from the center of a composite particle, shows a very weak amorphous ring pattern. However, with the increase of distance to the center of the composite particle, the diffraction patterns shows more and more distinct amorphous rings, as shown in Figs. 1f and 1g, which suggest that PANI–TiO_2 composite is composed of polycrystalline parts and amorphous parts. The polycrystalline parts distribute in the field near the surface of TiO_2

Table 1. The Characteristics of PANI–TiO_2 Composites

Sample No.	PANI content /wt%	Density /g·cm^{-3}	Conductivity /S·cm^{-1}	Color	Dimension /nm
S_0	100	1.16	1.36	bottlegreen	—
S_1	88.5	1.20	0.96	emerald	50—60
S_2	72	1.31	0.63	turquoise	50
S_3	53	1.72	0.39	aqua	40—45
S_4	39	2.04	0.19	celadon	30—35

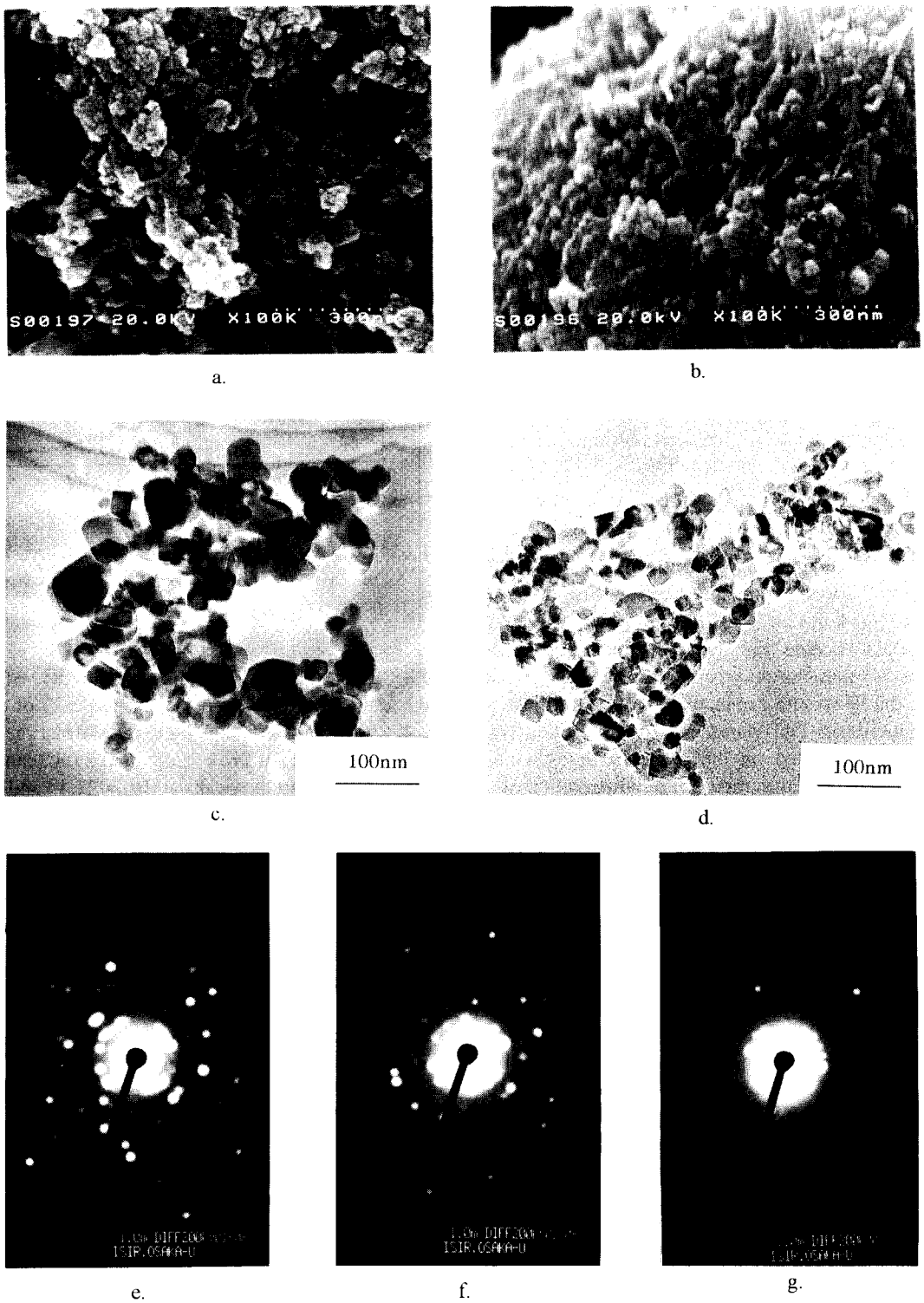

Fig. 1. SEM and TEM micrographs of PANI–TiO_2 nanocomposites. a. SEM image of S_1; b. SEM image of S_2; c. TEM image of S_2; d. TEM image of S_3; e. Diffraction pattern near the centre of particles of S_2: f. Diffraction pattern between centre and edge of particles of S_2; g. Diffraction pattern near the edge of particles of S_2.

and the amorphous parts distribute in the field far from the surface of TiO_2, which are due to the restrictive effecting of the surface of TiO_2 while polyaniline chains grow. Incontestably, the diffraction of TiO_2 itself contributing to Fig. 1e should also be considered.

Figure 2 shows the FTIR spectra of PANI and PANI–TiO_2 composites. The spectra A, B and C correspond to S_0, S_1 and S_2, respectively. Comparing between the spectra A, B and C, one can find some differences. Firstly, the peaks which appear broad in the spectrum A became more resolved to individual components in spectra B and C. Secondly, the intensities and shapes of some peaks upon introduction of

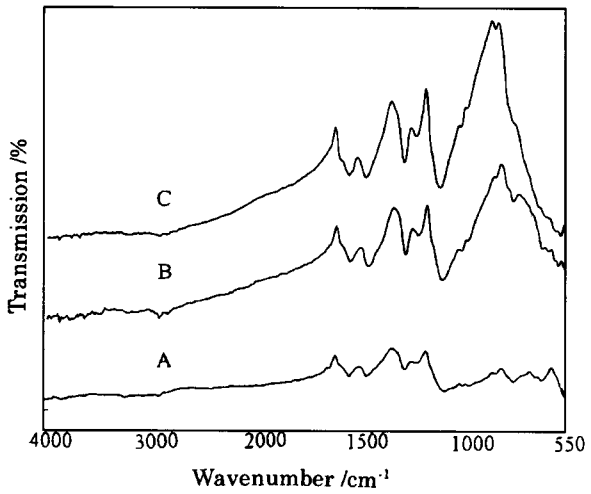

Fig. 2. FTIR spectra of PANI synthesized with and without TiO_2. Curve A, B and C correspond to S_0, S_1 and S_3, respectively.

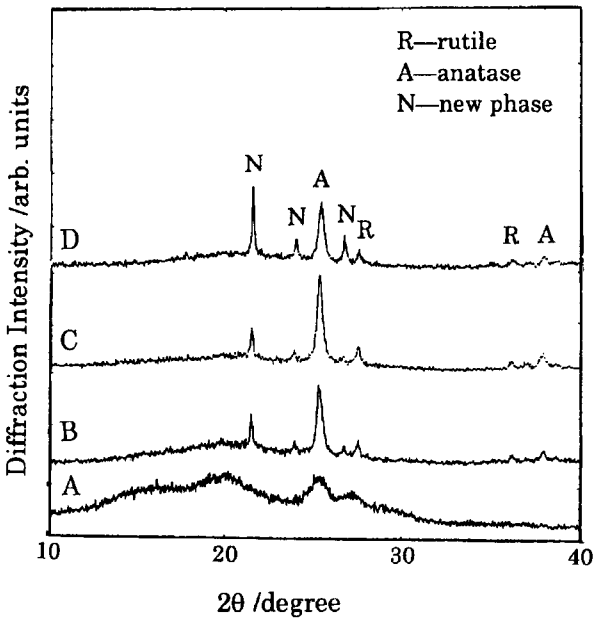

Fig. 3. X-ray diffraction patterns of S_0 (curve A) and S_1, S_2, and S_3 (curves B,C and D correspond to S_1, S_2 and S_3, respectively).

TiO_2 particles, for example at 2860, 1560, 1475, 1300, 1120, 1022 and 880 cm^{-1}, turn strong and sharp because of being affected by the presence of TiO_2 during PANI synthesis. Thirdly, the peaks became much sharper when more TiO_2 particles were put into the polymerization system. These differences in the IR spectra can be explained as follows.

Upon introduction of TiO_2 particles into the reaction system, aniline gets adsorbed on the oxide particles which were dispersed in the reaction mixture; polymerization proceeds initially on the surface of these oxide particles when $(NH_4)_2S_2O_8$ is added to the reaction system. DBSA acts in the roles of dopant and emulphor, which makes monomers disperse more uniformly. This leads to adhesion of the polymer to the TiO_2 particles and results in constrained growth around the particles. Such adsorption and constrained motion of the chains will restrict modes of vibrations in polyaniline, which will lead to the differences in the IR spectra. Sharpness of the peaks in the IR spectra and better resolution of the bands suggest that the composite particle size is small.

The X-ray diffraction patterns of pure PANI and PANI-TiO_2 composites are shown in Fig. 3. Curves A, B, C and D are corresponding to S_0, S_1, S_2 and S_3, respectively. In some earlier reports, PANI has been described as an amorphous polymer.[16] However, we have recently reported three broad peaks centring around 2θ = 20.2°, 25.3° and 27.2° in the XRD patterns of emulsion polymerized PANI doped with DBSA.[15] Study of the XRD patterns of the present samples also reveals some degree of crystallinity, with appearance of three broad peaks in the region of 2θ = 20—30°, with a maximum around 25.2° for PANI as shown with the curve in Fig. 3A. The peaks may be assigned to the scattering from PANI chains at the interplanar spacing. For the composites of PANI–TiO_2 with different TiO_2 content identical XRD patterns are observed as curves B, C and D in Fig. 3. When the PANI chains were stacked around TiO_2 particles, the broad weak diffraction peaks of PANI disappeared gradually, while new strong sharp diffraction peaks evolved at 2θ = 21.4°, 23.8°, 25.3°, 26.5°, 27.4°, 36.1° and 37.8° with increasing TiO_2 content in the composite. The peaks of 2θ = 25.3°, 27.4°, 36.1° and 37.8° belong to the diffraction of TiO_2 particles. The peaks at 2θ = 25.3° and 37.8° can be ascribed to the anatase and the peaks at 2θ = 27.4° and 36.1° to the rutile. The new peaks appear at 2θ = 21.4°, 23.8° and 26.5°, which means the existence of interactions between polyaniline and TiO_2. The components of these new phases are not well-known for the moment. During polymerization, the growth of PANI chain is interpreted to be restricted around TiO_2 particles and the polyaniline around the TiO_2 particles is in a crystalline state. With the increase of TiO_2 content in composites, these peaks become sharper and the amorphous scattering region reduces. It implies that the composite samples have a more ordered arrangement than the PANI, which is also reflected in their TEM images.

TGA is a useful method for testing the thermal stability of composites. Figure 4 shows a comparison of mass losses of PANI, TiO_2 and PANI–TiO_2 composites upon heating in air atmosphere. TiO_2 is very stable and no decomposition takes place in the range of 30—600 °C. Polyaniline displays a sudden decrease in mass of about 10% at the temperature 280 °C, which is corresponding to the breakaway of DBSA.[17] After that, a steady decrease in mass occurs in the range of 280—600 °C. Below 100 °C the decrease of mass is due to the release of a small part of water in the sample. PANI–TiO_2 composites exhibit good stability under air, showing a slight mass loss (about 4%) from 100 °C until 400 °C; after that the degradation rate increases. The mass loss at 600 °C is smaller in the composite with large TiO_2 content. Since the trend of degradation curve of PANI–TiO_2 composite is similar with that of PANI, the degradation of the PANI–TiO_2 composites is interpreted to be mainly controlled by the decomposition

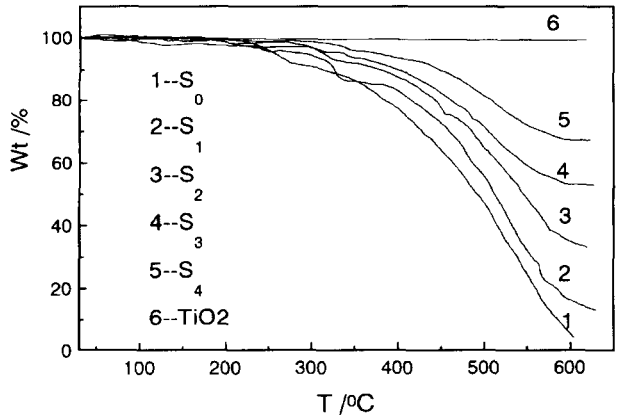

Fig. 4. Thermogravimetric analysis for PANI–TiO_2 composites containing different amounts of TiO_2 added in the reaction mixture. Curves 1 to 5 correspond to that of S_0, S_1, S_2, S_3 and S_4, respectively. Curve 6 corresponds to that of TiO_2.

of PANI.

From the TGA curves, we can evaluate the PANI content in the product. Table 1 indicates the characteristics of the samples containing different concentrations of TiO_2. It can be found in this table that the density of PANI–TiO_2 composite increases and the conductivity decreases with increasing TiO_2 content in composites. The increase of the density with increasing TiO_2 content is reasonable, because the specific weight of TiO_2 is much larger than that of PANI.

The conductivity of the composites is determined by the polyaniline of lower resistivity. In the conducting polymers composites, conductivity depends upon not only the doping level, conjugated length or chain length but also upon some external factors like compactness of the sample or orientation of the microparticles. In the present samples, PANI being polymerized in identical conditions other than the content of TiO_2, the conductivity values of the composites are determined by the effect of the TiO_2 on both conjugation length in PANI chain and the physical properties of PANI-TiO_2 composites. During the polymerization of polyaniline, TiO_2 particles dispersed in the reaction system act as the reaction cores, resulting in the adsorption of aniline on the surfaces of TiO_2 particles and subsequent formation of PANI. With the increase of the concentration of TiO_2, the effective surface area for reaction increases and the amount of anilines adsorpted on the surface of each TiO_2 particle decrease, giving rise to the polymerization degree dropping and the conjugation lengths decreasing which leads to the decrease of conductivity.

Furthermore, owing to the constrained and adsorption effect of the TiO_2 surface, the microscopical structure of composites is not uniform but is composed of orderly state and disorderly state; this is further supported by the TEM images of the composites. In this complicated morphology of the composite, the carrier transport may also be restricted at the boundary of particle, which leads to the decrease of conductivity in the sample of layer TiO_2 contact. Therefore, the reduction of the conjugation length in polymer chains and the complicated microscopic state of the composites result in the decrease of the conductivity of the composites.

Temperature dependences of conductivity of S_0, S_1 and S_4 are measured at temperatures between 200 to 290 K, the result is shown in Fig. 5. It is found that the conductivity values for all samples decrease with decreasing temperature, exhibiting typical semiconductor behavior. Conductivity of PANI–TiO_2 with larger TiO_2 content in composites has much stronger temperature dependence, which suggests that localization of charge carriers is greater in the composites with TiO_2 content increasing.[18] That is, by the addition of TiO_2 during polymerization, the effective conjugation length in PANI chains is shortened, which leads to the decrease of the delocalization of charge carriers. Macroscopical behavior exhibits the decrease of the conductivity of the composites.

To elucidate the photosensitive characteristics in PANI–TiO_2 composites, absorption spectra of pure PANI film and PANI–TiO_2 composite film were measured. The result is shown in Fig. 6. The absorption in both ultraviolet and visible region increased considerably due to the introduction of TiO_2 with the maximal absorption peaks at 318 nm. Owing to the addition of TiO_2 during polymerization,

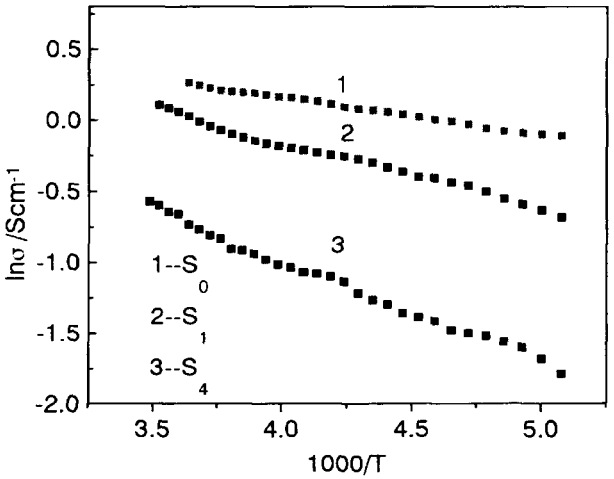

Fig. 5. Temperature dependence of conductivity of S_0, S_1, and S_3.

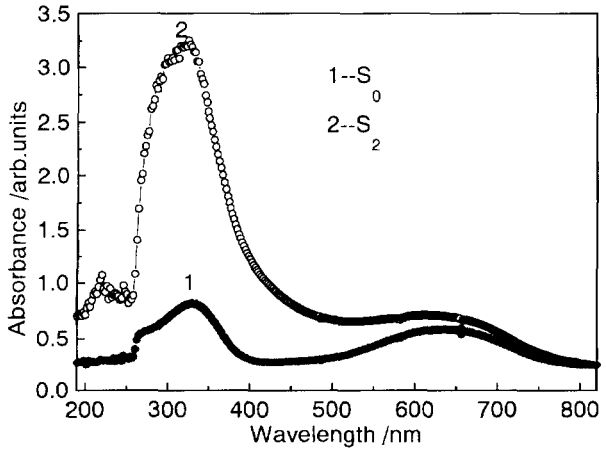

Fig. 6. Absorption spectra of S_0 and S_2.

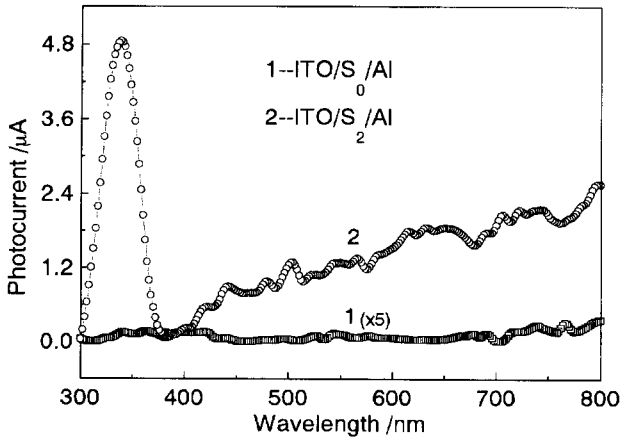

Fig. 7. Photoconductivity spectra of S_0 and S_2.

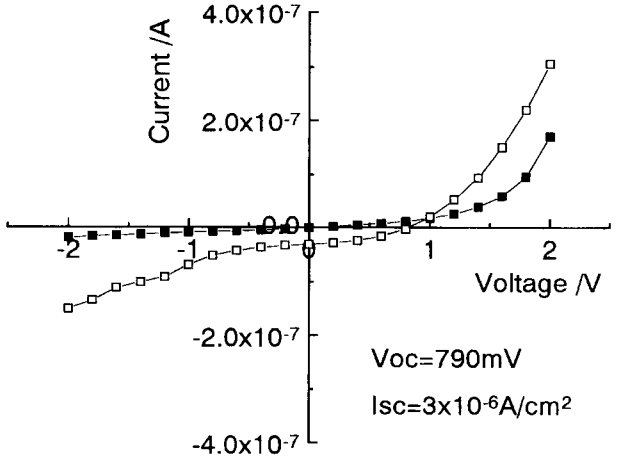

Fig. 8. Current-voltage characteristics of S_2 in the dark (■) and under illumination (□).

the spectrum becomes broader and the peak at 340 nm shifts to 318 nm. Moreover, the weak absorption of pure PANI at 400—600 nm has been improved distinctly, which is attributed to the improvement in morphology of PANI chains.

Photovoltaic measurements are made on the device with the structure ITO/PANI–TiO_2/ITO. The spectral response of the photocurrent for the PANI–TiO_2 composite film is shown in Fig. 7. For the sake of comparison, the photocurrent for ITO/PANI/Al(without TiO_2) is also shown in Fig. 7. The photocurrent of the PAN–TiO_2composite is two orders of magnitude higher than that found in PANI-only structures, which suggests the improved efficiency in exciton dissociation in the presence of TiO_2. It could be found that the highest peaks in photocurrent spectra appear at 337 nm which is corresponding with the absorption of TiO_2. Moreover, the photocurrent response of the composite is also improved markedly in the visible region.

A typical current-voltage curve corresponding to the photocurrent spectrum of PANI–TiO_2 composites is shown in Fig. 8. The device is irradiated with the monochromatic light of 344 nm in wavelength and 19.5 μW/cm^2 in intensity through the ITO electrode. The short-circuit current density is 3 μA/cm^2 with an open-circuit voltage of 790 mV. The improvement of the photocurrent of the PANI–TiO_2 composites can be explained as follows.

A photocurrent is generated when photons are absorbed by both PANI and TiO_2 at the PANI–TiO_2 interface in the composite film and the efficient charge separation takes place between PANI and TiO_2 in the composite film. That is, by the dissociation of the excitons at the interface, electrons should be transferred from PANI to TiO_2. After charge transfer has occurred, the charges can then travel to the respective electrodes driven by the internal electric field, which leading to the improvement in conversion efficiency.

Summary

Densely packed PANI–TiO_2 nanocomposites with relatively high conductivity values were synthesized by in situ emulsion polymerization and particle sizes could be controlled. TiO_2 particles were encapsulated in the cores of the growing polymer chains, resulting in the formation of an inorganic-organic hybrid material. Owing to this specific complex nanocomposite, the underlying change revealed itself in the improvement in different physical properties of PANI, such as its compactness and mechanical property, morphology, DC conductivity, thermal stability, crystallinity, density and photoconductivity. The mechanism of electrical transport in these materials was revealed by their conductivity and temperature-conductivity relation measurements, and the improvement of photoconductivity was discussed in terms of the photo-induced charge transfer. The improvements made in various physical properties of the present nanocomposite are expected to enhance the application potential of the conducting polymer without hampering its chemical properties.

References

1 A. P. Alivisatos, *Science*, **271**, 933 (1996).
2 Y. Wang and N. Herron, *Chem. Phys. Lett.*, **200**, 71 (1992).
3 J. J. M.Halls, C. A. Walsh, N. C. Greenham, E. A. Marseglia, R. H. Friend, S. C. Moratti, and A. B. Holmes, *Nature*, **376**, 498 (1995).
4 N. C. Greenham, X. Peng, and A. P. Alivisatos, *Phys. Rev.*, **B54**, 17628 (1996).
5 P. R. Somani, R. Marimuthu, U. P. Mulik, S. R. Sainkar, and D. P. Amalnerkar, *Synth. Met.*, **106**, 45 (1999).
6 Y. N. Xia, *Plast. Eng.*, **45**, 359 (1998).
7 T. A. Kerr, H. Wu, and L. F. Nazar, *Chem. Mater.*, **8**, 2005 (1996).
8 Y. J. Liu and M. G. Kanatzidis, *Inorg. Chem.*, **7**, 1525 (1993).
9 M. G. Kanatzidis and C. Wu, *J. Am. Chem. Soc.*, **111**, 4139 (1989).
10 M. X. Wan, W. X. Zhou, and J. C. Li, *Synth. Met.*, **78**, 27 (1996).
11 R. E. Partch, S. G. Gangolli, E. Matijevic, W. Cai, and S. Arajs, *J. Colloid. Interface. Sci.*, **27**, 144 (1991).
12 C. Dearmitt and S. P. Armes, *Langmuir*, **9**, 652 (1993).
13 L. M. Gan, L. H. Zhang, H. S. O. Chan, and C. H. Chew, *Mater. Chem. Phys.*, **40**, 94 (1995).
14 Y. Haba, E. Segal, and Narkis, *Synth. Met.*, **106**, 59 (1999).
15 Feng Wei, Wei Wei, and Wu Hongcai, *Chem. J. Chin. Univ.*, **20**, 318 (1999).

16 W. R. Salaneck, D. T. Clark, and E. J. Sanuelsen, "Science and Applications of Conducting Polymers," Adamhiger, New York (1990), and references therein.

17 Feng Wei, Wei Wei, and Wu Hongcai, *Journal of functional polymers*, **11**, 237 (1998).

18 K. Yoshizawa, A. Ito, K. Tanaka, and T. Yamabe, *Solid State Commun.*, **87**, 935 (1993).